Title | Rhythmic Coordination between the Dentate Gyrus (DG) and CA3 During a Spatial Pattern Separation Task

Background | We are inherently able to discriminate between highly similar sensory inputs and utilize a complex understanding of subtle differences in spatial locations to distinguish between seemingly identical objects. Within the medial temporal lobe (MTL), the hippocampal formation (HF) and parahippocampal region (PHR) have been widely attributed to the cognitive functions of learning and memory that guide these inherent abilities. The HF is composed of many subregions: the dentate gyrus (DG), CA3, CA2, CA1, and subiculum[1]. Although each of these subregions is believed to contribute in a unique manner, communication between them is thought to be essential to learning and memory processes. Of these subregions, studies have demonstrated that it is the DG that is required for discriminating between highly similar sensory inputs. At the cellular and network level, it is hypothesized that this is accomplished through "pattern separation" in which similar multimodal sensory inputs from the Entorhinal Cortices (EC) engage the activity of distinct, or orthogonal, populations of DG granule cells [2,3]. Distinct representations of experience in DG are then strongly outputted downstream to the CA3 subregion of the HF. Although lesion studies have provided evidence for this function of DG, we aim to improve the understanding of the functional contributions of this specific subregion using *in vivo* electrophysiology to assess the neural activity of both single cells and local field potential (LFP) during task-relevant processing.

Rhythmic interactions between hippocampal neurons can create temporal windows of inhibition and greater excitability that enable cells to flexibly select or ignore inputs[4]. These rhythmic interactions can have stereotyped time courses, manifesting in the LFP as neural oscillations with unique frequency bands. For this reason, the study of neural oscillations during behavior can provide insight into the rhythmic interactions and the temporal organization of spiking activity that facilitates task-relevant information processing[5,6]. **Aim 1. Characterize the rhythmic profile of the DG and CA3 subregions during a spatial pattern separation task**. Assess how the different spatial separations (i.e. close arms, far arms) may engage distinct rhythmic interactions, as observed from the LFP. Distinct profiles may suggest that different rhythmic interactions are required to adequately organize the local activity in a specific way to allow successful completion of the task. Furthermore, by comparing simultaneous recordings from multiple HF subregions, such as both DG and CA3, it is possible to uncover the timing and underlying mechanisms of cross-regional communication that is required for successful task performance. **Aim 2. Analyze the coherence of rhythmic profiles between subregions of DG and CA3 in order to assess when they are potentially communicating.**

Methods | A single Long-Evans rat will be used as the subject in this study. The test apparatus for the spatial pattern separation task was a 14-arm Fan Maze (Figure 1a). Each trial began with a *sample* phase in which the rat was released from the start box, ran down the single *home* arm, and stopped at the choice point (the end of the *home* arm before the central arena). He then visually scanned for the single Lego object that covered a baited food-well at the end of one of the 14 radial arms. The rat was trained to run down that arm to displace the Lego object in order to reveal his food reward (i.e. honey-nut cheerio) and then return to the start box. Following this was the *test* phase in which the Lego object was placed over the same baited food-well from the *sample* phase while an additional identical Lego object, known as the foil object, was placed over an unbaited food-well of a different arm. The arm containing the unbaited foil object was pseudorandomly chosen to be in one of two locations: covering the food-well of an arm adjacent to that of the *sample* phase (close condition) or a food-well that was 7 arms away (far condition). Once the rat was released from the start box, he could either correctly run down the arm from the *sample* phase to attain the food reward or incorrectly visit the novel arm with the unbaited foil object. After choosing one of the arms, the rat returned to the start box which marked the end of the trial. Each recording day consisted of 40 or 80 counterbalanced, pseudorandom trials in order to avoid over-exposure to any single arm or arm combination. Neural data was obtained by implanting a Microdrive recording device with 24 independently moveable tetrodes that were progressively lowered into the hippocampal subregions of interest (Figure 1b).

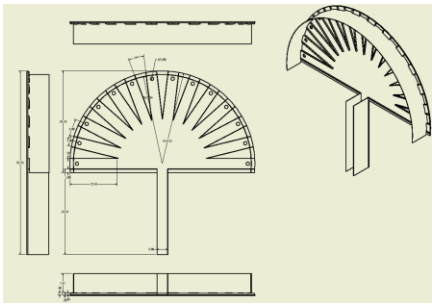

Figure 1a. Fan Maze

Figure 1b. Microdrive

Schematic of the 14-arm test apparatus, Fan Maze, used in the spatial pattern separation task (Figure 1a). Microdrive with 24 independently moveable tetrodes used to perform the *in vivo* electrophysiological recordings (Figure 1b).

Results | The data analysis was performed on neural data acquired from three days of simultaneous *in vivo* electrophysiological recordings in the DG and CA3 hippocampal subregions. These days consisted of at least 60% success rates throughout the entire recording session. When the rat performed the close condition correctly, the Gabor amplitude spectrogram demonstrated an increase of amplitude in the beta (15-30 Hz) frequency range in the DG shortly after the rat encountered the Lego object (Figure 2a). This shift in frequency was not present in the DG when the rat incorrectly performed the close condition, but rather an amplitude increase in the theta (4-12 Hz) frequency range was shown (Figure 2b). Furthermore, recordings from the CA3 during correct-close conditions demonstrated a similar increase of amplitude in the beta frequency range with the addition of increases in low gamma (35-55 Hz) frequencies shortly after the rat encountered the object (Figure 2c). Incorrect-close conditions resulted in small bursts of increased beta amplitude after the object encounter (Figure 2d). Surprisingly, the spectrograms for the far condition demonstrated the same patterns of frequency shifts across the correct vs. incorrect trials (Figure 3a-d).

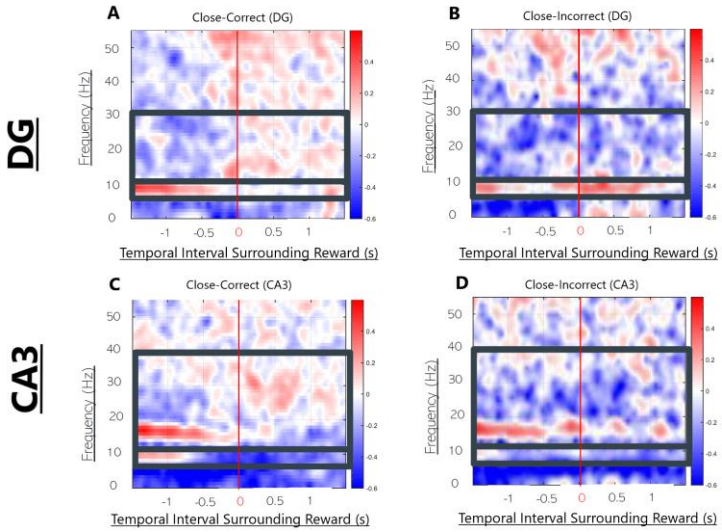

Figure 2. Amplitude spectrograms averaged across the three recording sessions for the close-condition *test* phases. Changes in theta (4-12 Hz), beta (15-30 Hz) and low gamma (35-55 Hz) amplitude during the time interval surrounding object encounter (marked as the central red line on the x-axis). Using the rhythmic profile of the object encounter as a baseline reference, red colors indicate an intensity increase in that frequency range at that given time, while blue indicates a decrease in that frequency's intensity; white means no change from baseline. (a) Frequency amplitude changes observed in the DG during Close-Correct trials. (b) Frequency amplitude changes observed in the DG during Close-Incorrect trials. (c) Frequency amplitude changes observed in the CA3 during Close-Correct trials. (d) Frequency amplitude changes observed in the CA3 during Close-Incorrect trials.

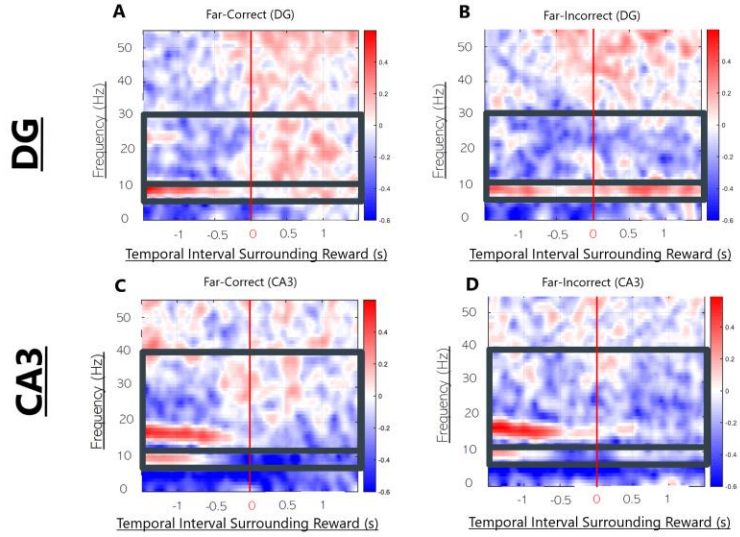

Figure 3. Amplitude spectrograms averaged across the three recording sessions for the far-condition *test* phases. (a) Frequency amplitude changes observed in the DG during Far-Correct trials. (b) Frequency amplitude changes observed in the DG during Far-Incorrect trials. (c) Frequency amplitude changes observed in the CA3 during Far-Correct trials. (d) Frequency amplitude changes observed in the CA3 during Far-Incorrect trials.

To assess possible communication between the DG and CA3 subregions, the percent coherence was plotted against the frequency ranges of interest for both one second before (pre-reward) and one second after (post-reward) encountering the object in all conditions (i.e. close-correct, close-incorrect, far-correct, far-incorrect). A percent coherence of one would indicate that the two electrical signals are perfectly aligned and that one could be predicted from another. Instances of non-overlapping standard error lines preliminarily indicated that there may be a difference in coordination between DG and CA3 across these instances, which are marked by grey bars below the line graphs. When comparing DG-CA3 coherence in close-correct and far-correct conditions, the pre-reward of the close-correct condition had a decreased coherence in the beta frequency range and the post-reward of this condition had an increased coherence in the beta range (Figure 4). While analyzing the correct and incorrect trials for only the close condition, the pre-reward of the correct trials had decreased beta coherence as well as decreased coherence in the low gamma range and the post-reward of the correct trials had increased coherences in those frequency ranges (Figure 5). The comparison of the correct and incorrect trials for the far condition demonstrated an increased coherence in the beta range during pre-reward of the correct trials, whereas the post-reward of the correct trials exhibited decreased coherence in low frequency ranges but increased coherence in the beta range (Figure 6).

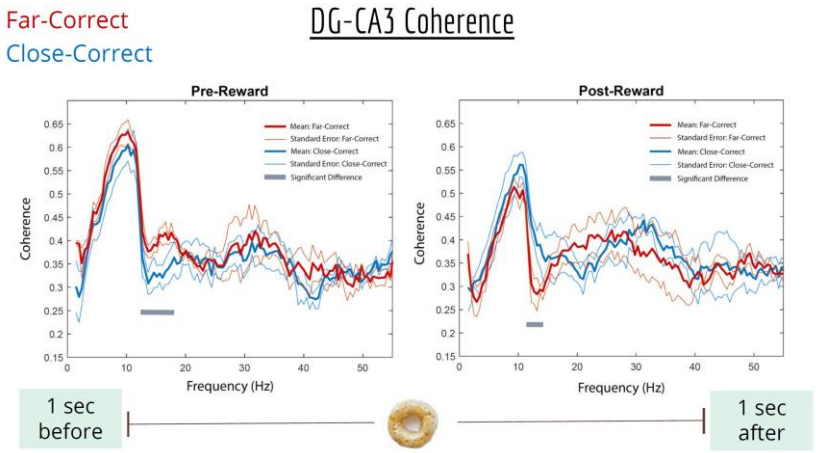

Figure 4. Percent coherence between DG and CA3 plotted against the frequency ranges of interest in which a coherence of one would indicate perfectly aligned signals. Mean coherence represencted as bold lines and standard errors represented by surrounding thin lines. During the Close-Correct (blue) and Far-Correct (red) conditions. Analyzed at two separate instances in time: one second prior to object encounter (left) and one second after object encounter (right).

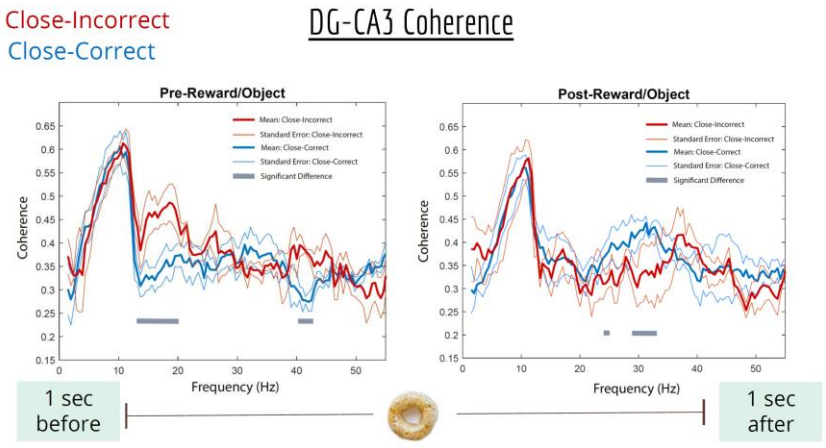

Figure 5. Percent coherence between DG and CA3 during the Close-Correct (blue) and Close-Incorrect (red) conditions. Analyzed at two separate instances in time: one second prior to object encounter (left) and one second after object encounter (right).

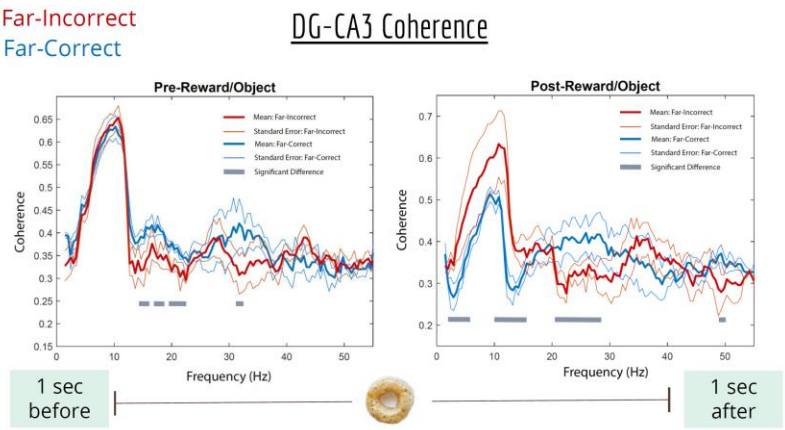

Figure 6. Percent coherence between DG and CA3 during the Far-Correct (blue) and Far-Incorrect (red) conditions. Analyzed at two separate instances in time: one second prior to object encounter (left) and one second after object encounter (right).

Discussion | In both DG and CA3, increases in high frequency oscillations (>15 Hz) are observed concomitantly with decreases in low frequency oscillations (~7-10 Hz) upon object approach/reward consumption during correct trials, but not incorrect trials. During object approach/reward consumption, decreases in coherence in the beta frequency range are observed between DG and CA3 during close-correct trials, but not during far-correct and incorrect trials. After object approach/reward consumption, increases in coherence in higher frequency ranges (>15 Hz) are observed between DG and CA3 during correct trials. Therefore, a difference between the close-correct and far-correct conditions is observed when comparing DG-CA3 coherence pre-reward. This preliminary suggested difference in coordination between subregions may be important in the ability to perform the spatial pattern separation task with an intact DG and lesioning the DG may affect this necessary component of cognitive processing. However, this preliminary data is based on an extremely small sample size (n=1) and cannot be used to analyze for statistical significance.

Future Directions | Larger sample sizes in the future will allow for a more statistically accurate representation of the neural data. Additionally, analyzing the data at multiple time intervals (i.e. during the *sample* phases), rather than solely during the *test* phases, will allow for a more complete understanding of the task-relevant processing and neural encoding progression. As for the methods of analysis, although the mean coherence preliminarily suggested coordination across subregions for certain conditions of the task, this suggested coherence does not necessarily indicate a direct relationship between the two subregions. Rather, it suggests that the rhythmic profile of the CA3 may possibly be predicted from the rhythmic profile of the DG at those points in time. However, comparing the spike-timing of CA3 cells to the LFP of DG may additionally uncover the degree to which rhythmic activity in DG influences CA3 spiking activity.

Acknowledgements | I would like to thank the entire staff of Neural Crossroads Laboratory for helping during every step of this year long process (i.e. discussing and sharing research articles, troubleshooting MATLAB data analysis, hosting practice talks, etc.). A special thanks to Dr. Lara Rangel, Pamela Riviere, and Teryn Johnson for sharing their expertise in this field of electrophysiology and data analysis. And lastly, to Dr. Marta Kutas for dedicating time weekly to overseeing the progression of the presentations.

References |

1. Van Strien N. M., Cappaert N. L. M. & Witter M. P. (2009) *Nature Reviews*. **10**, 272-282.
2. Gilbert P.E., Kesner R.P. & Lee I. (2001) *Hippocampus* **11**(6), 626-636.
3. Piatti V. C., Ewell L. A. & Leutgeb J. K. (2013) *Frontiers in Neuroscience*. **7**(50).
4. Fries P. (2005) *TRENDS in Cognitive Sciences*. **9**(10), 474-480.
5. Cannon J. et al. (2014) *European Journal of Neuroscience*. **39**, 705-719.
6. Rangel L., Chiba A. & Quinn L. (2015) *Frontiers in Systems Neuroscience*. **9**(96).